**SIRM 2015 – 11th International Conference on Vibrations in Rotating Machines,
Magdeburg, Germany, 23. – 25. February 2015**

Torsional Vibration Problem in Reciprocating Compressor – Case Study

Fikre E. Boru (Dr.-Ing.)[1], **Johann Lenz (Dr.-Ing.)[2]**

[1] Machinery and Plant, KÖTTER Consulting Engineers GmbH & Co. KG, Rheine, Germany,
Fikre.Boru@koetter-consulting.com
[2] Machinery and Plant, KÖTTER Consulting Engineers GmbH & Co. KG, Rheine, Germany,
Johann.Lenz@koetter-consulting.com

Abstract

Reciprocating compressors are unavoidable classical solutions in the field of natural and process gas compression with the ability to function over a wide range of operating conditions. The dynamic design of the reciprocating compressor is complicated due to the large number of conditions that have to be fulfilled. Since high torsional dynamic stress is often not recognized until damages appear, it is advisable to conduct a detailed torsional vibration analysis when planning a new drivetrain or modifying an existing one.

In the effort to adapt to the varying demand of the market, natural and process gas facilities revamp fixed speed reciprocating machines with variable speed drive (VSD) and (active) suction valve unloading devices. Such a revamp leads to a change (often to the worst) of the dynamic behavior of the drivetrain even though the components in the train remain unchanged.

The motivation of this article emanates from a practical example, where the torsional vibration of a reciprocating compressor after installing of a stepless active suction valve unloader led to repeated failures of the coupling. The purpose of this paper is to raise awareness of torsional vibration problems and to outline an analytical procedure to follow in the design stage (new or revamp).

A finite-element-model of the complete drivetrain including the non-linear rubber coupling and the periodic excitation torque (inertial and gas forces) is developed. As will be shown in the paper, the resulting equation of motion of the drivetrain is a second order differential equation with operation dependent damping matrix. The solution to the differential equation is then solved in the time domain. In the described practical example, the analytical and the measurement results are compared with each other. Then, a list of practical recommendations based on experience is provided to tame the torsional vibration problem during operation.

Nomenclature

K_a	-	equivalent stiffness of non-circular section
K_b	-	stiffness of the base shaft
T	-	thickness of the arm
D_S	-	diameter of the circumscribing circle of the non-circular shaft
D_b	-	diameter of the base shaft
λ	-	web construction parameter (= 1 for intergral construction, < 1 for welded construction
m_p	-	piston and piston rod mass
a_p	-	piston acceleration
p_{ie}	-	internal, external cylinder pressure
A_{ie}	-	internal, external piston area
K_t	-	torsional stiffness of crankshaft
G	-	modulus of rigidity
L_j	-	length of journal
L_W	-	length of crank web
L_C	-	length of crankpin
D_j	-	outer diameter of journal
d_j	-	inner diameter of journal
D_C	-	outer diameter of crankpin
d_C	-	inner diameter of crankpin
D_C	-	outer diameter of crankpin
W	-	width of web
R	-	throw radius
$\mathbf{m_j}$	-	element torsional inertia matrix
$\mathbf{c}_\varphi$	-	element torsional damping matrix
$\mathbf{k_t}$	-	element torsional stiffness matrix
J_p	-	polar moment of inertia of an element about the rotational axis
c_φ	-	torsional damping of an element

k_t	-	torsional stiffness of an element	α	-	crankshaft angular displacement
$\mathbf{M_j}$	-	global torsional inertia matrix	T_{cs}	-	torque load on crankshaft
$\mathbf{C}_{\varphi}$	-	global torsional damping matrix	F_{osc}	-	dyn. forces of the oscillating crosshead and connection rod masses
$\mathbf{K_t}$	-	global torsional stiffness matrix	F_p	-	piston rod force
$\vec{T}$	-	global excitation torque vector	ψ	-	relative damping
$\vec{\alpha}$	-	vibratory angular displacement vector	Ω	-	rotational velocity

1 Introduction

In the field of natural and process gas compression reciprocating compressors are preferable choices due to their ability to function over a wide range of operating conditions. Since their failure is associated with substantial financial loss and possible loss of human life, the required level of reliability is very high. Hence a detailed analysis, for example a torsional analysis, is required in the design phase of these machines.

In the torsional analysis of reciprocating compressors all parts in the drivetrain have to be considered. A typical compressor comprises of a crankshaft, an optional flywheel, a coupling and driving unit (with or without gear). In addition to the above mentioned parts some compressor manufacturers couple auxiliary pumps to the non-drive end of the crankshaft.

Unlike lateral and axial vibration, torsional vibration is not simply perceivable unless elements in the drivetrain lead to a coupled lateral vibration. The measurement of torsional vibration requires the use of either strain gauges or optical instruments in contrast to lateral vibrations which can be measured using readily available sensors. Hence, torsional dynamic stress is often not recognised until damages appear.

There are plenty of literature and books discussing torsional analysis in mechanical systems, some of these discuss the torsional vibration of reciprocating machines. However, due to a combination of inaccurate considerations in design and inexperience the torsional problem in reciprocating machines still remains large. The following literature is particularly recommended to those interested in the torsional analysis of reciprocating machines [1, 4, 6, 7, 10 and 12].

2 Modelling of the reciprocating drivetrain

The dynamic analysis of any mechanical system starts with the mathematical modelling of the mass-elastic system. In this section a set of simplified equations are given for the determination of the mass-elastic properties of the reciprocating compressor drivetrain. In this paper a reciprocating compressor driven by an electric induction motor, coupled by a typical elastic coupling and having a flywheel is discussed. Figure 1 shows a representative sketch of a typical reciprocating compressor.

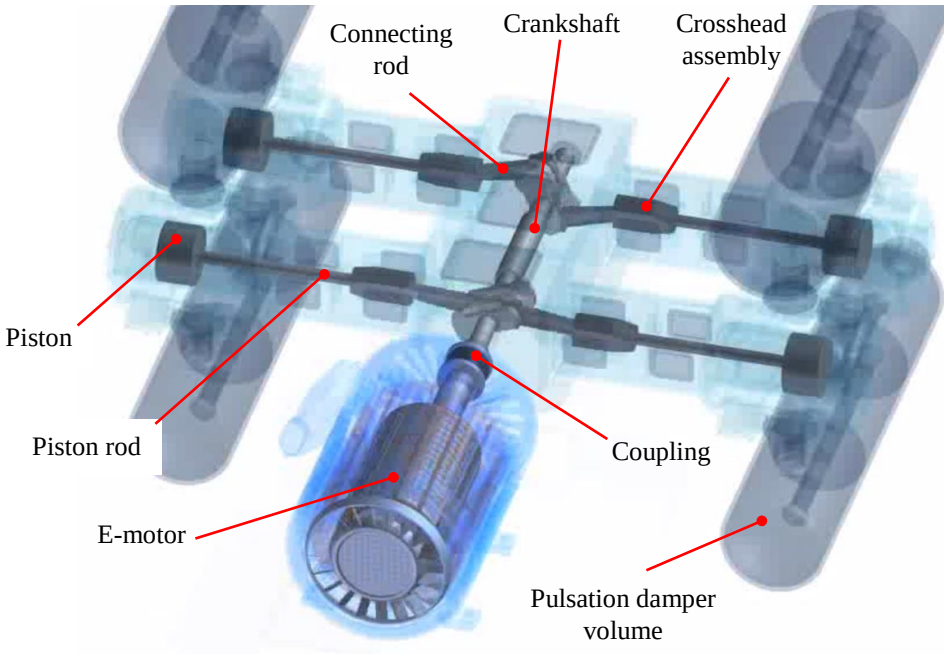

Figure 1: Representative sketch of a typical four cylinder reciprocating compressor.

2.1 Electric motor

An induction electric motor is composed of a combination of simple circular shafts (with or without keyways) and non-circular section at the motor winding (circular section with radial webs). The determination of the polar inertia is relative simple but the exact torsional stiffness of such sections is complicated. Equation (1) gives a simplified relation for the determination of the torsional stiffness of typical cross-sections used in electric motors as given in API 684 [1]. Isakower [9] listed the torsional properties of a number of non-circular cross-sections. The polar inertia and torsional stiffness can also be numerically estimated using the finite-element-method when the exact technical drawing (which is not always easily to get) is supplied by the motor manufacturer. The "rough" technical drawing supplied by motor suppliers usually contains the total shaft polar moment of inertia, the polar moment of inertia of assembled parts such as the motor windings and cooling fans as well as the torsional stiffness of the motor shaft between two points. Based on this information, which according to our experience is accurate enough for the torsional analysis, the mass elastic properties can be determined.

$$\frac{K_a}{K_b} = \frac{\lambda\left[1+\dfrac{24TL}{\pi D_b^2}\right]}{1+\dfrac{16TL^3}{\pi D_b^4}\left[1+\left(\dfrac{T}{D_S}\right)^2+3\left(1+\dfrac{D_b}{D_S}\right)^2\right]} \tag{1}$$

2.2 Coupling

Couplings are devices for joining two rotating shafts semipermanently at their ends so as to transmit torque from one to the other. In addition to torque transmission couplings usually compensate for axial and radial misalignment between the two shafts. In reciprocating compressor drivetrains couplings can be classified into two general classes – rigid-flexible disc coupling and torsionally-soft elastomeric coupling.

Rigid-flexible disc couplings require no lubrication and maintenance, have high torsional rigidity and can operate in high temperature environment. But these couplings lead to a relatively high fundamental torsional natural frequency with interferences with the excitation frequencies and provide no damping to the drivetrain.

On the other hand torsionally-soft elastomeric couplings add additional damping in drivetrain, isolate excitation between components in the drivetrain and have a low fundamental torsional natural frequency with no interference with the excitation frequency. The main disadvantage of elastomeric couplings is the limited life of rubber elements due to heat generation. Hence, elastic couplings with flywheels are usually used in reciprocating compressor drivetrains. Feese and Hill [6] discussed a number of torsionally soft couplings and presented their advantages and disadvantages.

In the particular case presented here, a single-row and multi-row rubber coupling are shown. The stiffness, the torque transmission, the allowable vibratory torque and the allowable thermal loading of the applied elastomer are usually given in the coupling catalogues. In some particular cases the mass-elastic data of the couplings are also supplied by the manufacturer.

2.3 Crankshaft

A typical simplified method for the determination of the mass elastic properties of the crankshaft is to follow the procedure outlined in API 684 [1]. Usually the finite-element-line-model of the crankshaft is modelled with the nodes at the throws and with torsional stiffness between the throws. The torsional stiffness of the crankshaft between the throws can be estimated with adequate accuracy using equation (2). This is an average of the Carter's and Ker Wilson's formulae [10]. The variables in this equation are depicted in the simplified sketch of figure 2 of a typical reciprocating compressor's crankshaft.

$$K_t = \frac{\pi G}{64}\cdot\frac{\dfrac{2L_j+0.4D_j+0.8L_w}{D_j^4-d_j^4}+\dfrac{1.75L_c+0.4D_c}{D_c^4-d_c^4}+\dfrac{2.5R-0.2\left(D_j+d_j\right)}{L_wW^3}}{\left[\dfrac{L_j+0.4D_j}{D_j^4-d_j^4}+\dfrac{L_c+0.4D_c}{D_c^4-d_c^4}+\dfrac{R-0.2\left(D_j+d_j\right)}{L_wW^3}\right]\cdot\left[\dfrac{L_j+0.8L_w}{D_j^4-d_j^4}+\dfrac{0.75L_c}{D_c^4-d_c^4}+\dfrac{1.5R}{L_wW^3}\right]} \tag{2}$$

The polar mass moment of inertias lumped at the throws can be determined by summing the mass moment of inertia of the two journal halves, the crankpin, the two webs, the part of the connecting rod (usually estimated to be two-third of the connecting rod total mass) and half of the reciprocating mass, which is assumed to be lumped on the crankpin, about the rotational axis. The reciprocating masses comprise part of the connecting rod (usually estimated to be a third of the connecting rod total mass), the piston-rod assembly, the crosshead assembly and any additional reciprocating mass.

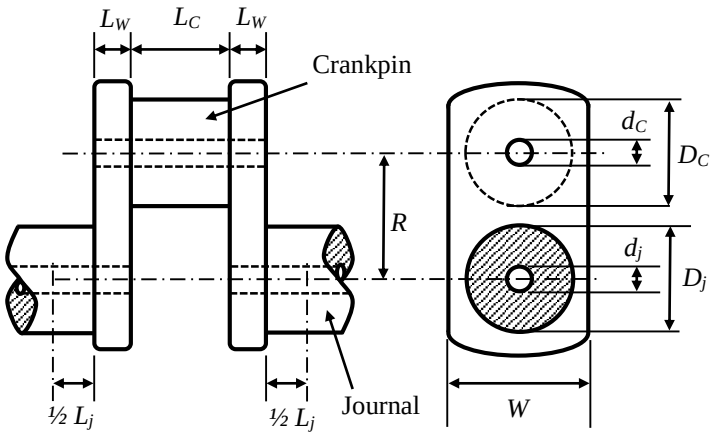

Figure 2: Simplified sketch of reciprocating compressor crankshaft.

The above stated physical parameters can be numerically estimated using the finite-element-method when the exact technical drawing is available. Here too some reciprocating compressor manufacturers supply the mass-elastic data instead of technical drawings from which the inertia and stiffness can be calculated. Experience shows that the data supplied from reciprocating compressor manufacturers are highly accurate.

3 Exciting torque of reciprocating compressor drivetrain

As presented in section two, the determination of the mass-elastic data of a reciprocating compressor drivetrain is simple. Technical documents and manufactures give enough information from which the physical parameters of the drivetrain can be estimated. From this information the torsional natural frequencies can be determined with acceptable accuracy. The parameters, which are difficult to determine, are the torsional damping and all sources of excitation in the drivetrain. In this section the main source of excitation is discussed.

The working principle of the reciprocating compressor leads to torsional excitation in the crankshaft. This torsional loading is then transmitted to the optional flywheel, the coupling and the driving motor. Besides the working principle of the compressor, a lot of factors influence the torsional loading of the drivetrain. The excitation loads responsible for the torsional fatigue loading are explained below.

The piston rod force F_P can be calculated from the cylinder gas forces and the simplified dynamic forces of the piston and piston rod masses as in equation (3). Unlike the dynamic forces, which are influenced by the moment of inertia of the reciprocating elements and the rotational speed only, the cylinder gas forces depend on a number of factors. The pressure in the cylinder including the acoustic pulsations are generated using an acoustic model which considers the cylinder design, the suction and discharge valve design, the discharge volume control mechanism, the properties of the compressed medium, the planned operation point of the compressor etc. One way to regulate discharge volume is the implementation of an active suction valve unloader, where the suction valve is actively maintained open during the compression phase to reduce the discharge volume.

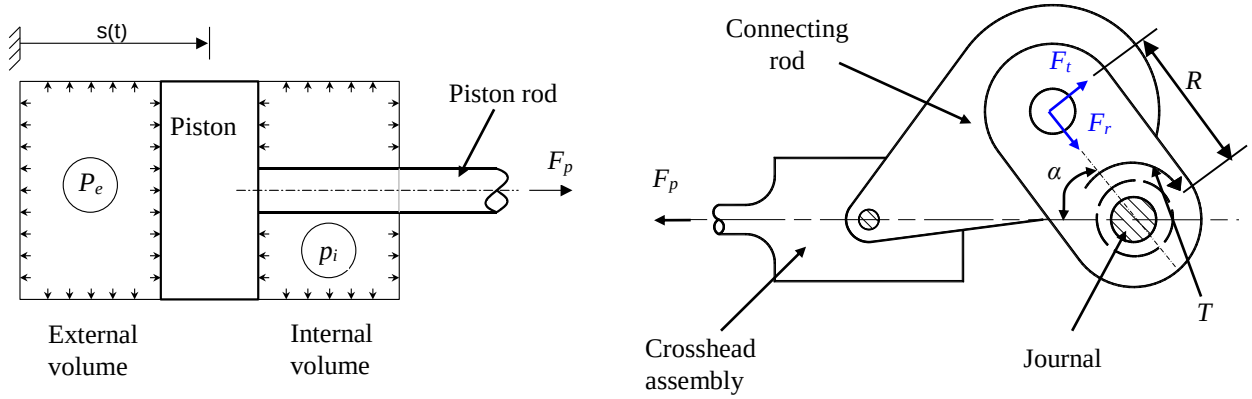

Figure 3: Simplified sketch of the cylinder (left) and section of the crankshaft, the connecting rod and the crosshead assembly (right).

$$F_p(\alpha) = m_p \cdot a_p(\alpha) + p_i(\alpha) \cdot A_i - p_e(\alpha) \cdot A_e \tag{3}$$

From the piston rod force F_p and the dynamic force of the crosshead and the reciprocating mass of the connecting rod (F_{osc}) one can calculate the radial force F_r and tangential forces F_t (as a function of the crankshaft angle α) acting on the crosshead pin. The crankshaft angle $\alpha(t)$ (here written as α for simplicity) is a function of time. Equation 4 gives the torque loading as a result of the tangential force component.

$$T(\alpha) = R \cdot \left(F_p(\alpha) + F_{osc}(\alpha)\right) \tag{4}$$

Figure 4 depicts the piston rod force and the resultant moment load of a single crankshaft of a typical slowly rotating natural gas reciprocating compressor for one complete crankshaft revolution.

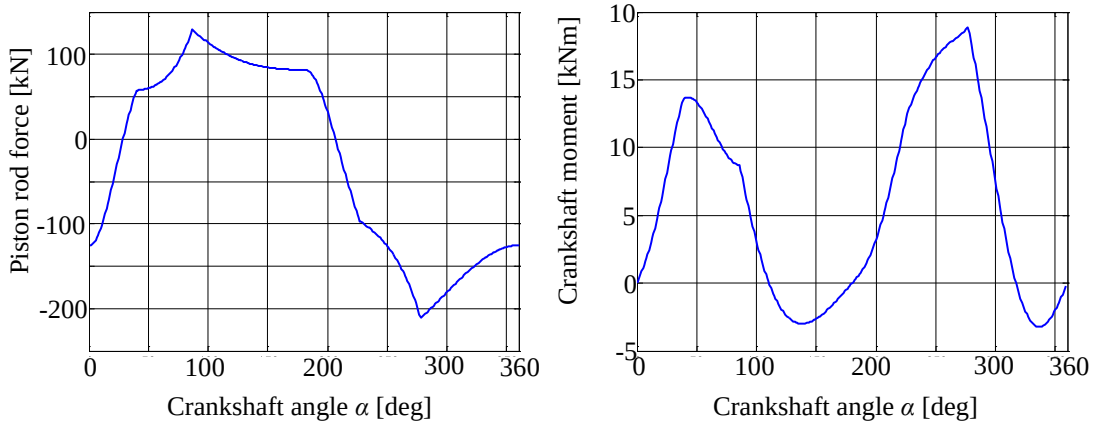

Figure 4: Calculated piston rod force and crankshaft moment, variation of a typical natural gas piston compressor as a function of crank angle for one complete revolution of the crankshaft.

In order to analyse the resulting torsional vibration, the spectrum of the dynamic components of the torque is generated as shown in figure 5.

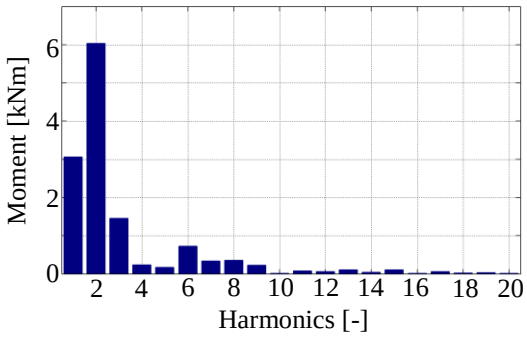

Figure 5: Spectrum of excitation torque.

The torque spectrum is composed of a number of harmonics which are multiples of the compressor rotational speed. The value of these harmonics depends on the operating condition of the compressor.

4 Torsional analysis

The components in the drivetrain can be subdivided into a number of finite elements. From the polar moment of inertia, the torsional damping and the torsional stiffness of the elements, the element torsional inertia matrix, torsional damping matrix and torsional stiffness matrix can be determined as shown in equation (5).The works of Argyris [2] and Irretier [8] has been followed in this paper for the formation of the FE-models.

$$\mathbf{m_j} = \frac{J_p}{6}\begin{bmatrix} 2 & 1 \\ 1 & 2 \end{bmatrix};\ \mathbf{c}_\varphi = c_\varphi \begin{bmatrix} \frac{1}{2} & 0 \\ 0 & \frac{1}{2} \end{bmatrix} \text{ and } \mathbf{k_t} = k_t \begin{bmatrix} 1 & -1 \\ -1 & 1 \end{bmatrix} \tag{5}$$

The element matrices ($\mathbf{m_j}$, $\mathbf{c_\varphi}$ and $\mathbf{k_t}$) are then assembled in the global matrices ($\mathbf{M_j}$, $\mathbf{C_\varphi}$ and $\mathbf{K_t}$) which form a system equation of motion. The equation of motion can be written in matrix form as follows:

$$\mathbf{M}_j\ddot{\vec{\alpha}} + \mathbf{C}_\varphi\dot{\vec{\alpha}} + \mathbf{K}_t\vec{\alpha} = \vec{T}(\alpha) \tag{6}$$

Torsionally soft couplings in reciprocating compressors usually use rubber elements which have constant relative damping ψ. The resulting damping matrix is therefore a function of the rotational velocity (see equation (7)), which in turn is influenced by the torsional vibration. Hence equation (6) is a non-linear differential equation of the second order. Beside the non-linear element matrices, the excitation gas forces are non-linear in nature that depend on operating pressure and temperature, volume flow, compressed medium, design of pulsation abating devices, number and design of cylinder valves etc.

$$c_\varphi = \frac{k_t\psi}{2\pi\ \Omega} \tag{7}$$

4.1 Modal analysis

The first step in the torsional analysis of a drivetrain is the determination of the homogenous solution of equation (6), i.e. the determination of the torsional natural frequencies and their corresponding mode shapes. Then the natural frequencies are plotted in a Campbell diagram along with the excitation orders. In the Campbell diagram the interference between the natural frequencies and the excitation orders, i.e. possible resonances, can be seen.

4.2 Transient analysis

When a reciprocating compressor operates over a wide speed range, it is almost impossible to avoid interference between excitation orders and all natural frequencies. But every resonance is not necessarily excited to high torsional vibration, depending on the excitation torque, system damping and location of excitation. Hence, the expected torsional vibration is determined through torsional response analysis, i.e. solving the non-homogenous equation. This analysis can be done both in frequency and in time domain. We prefer here to conduct the analysis in the time domain, especially when dealing with drivetrains with rubber couplings and operating over a wide speed range to incorporate the non-linear behavior of the system. Dukkipati [5] discusses different methods of solving second order differential equations by direct numerical integration.

5 Case study

5.1 Problem statement and task description

Next, the case study of a variable speed natural gas reciprocating compressor (600 rpm to 996 rpm) is presented. The drivetrain of this single-stage compressor comprises a 1.8 MW asynchronous motor and an elastic coupling with a moderate flywheel. After about 8 years of operation, the compressor was retrofitted with an active stepless suction valve unloading device on the head end cylinders in order to allow lower volume flow at minimum speed. This modification was deemed necessary to extend the delivery range of the plant. A couple of months after the retrofit a coupling failure led to drivetrain downtime (see figure 6).

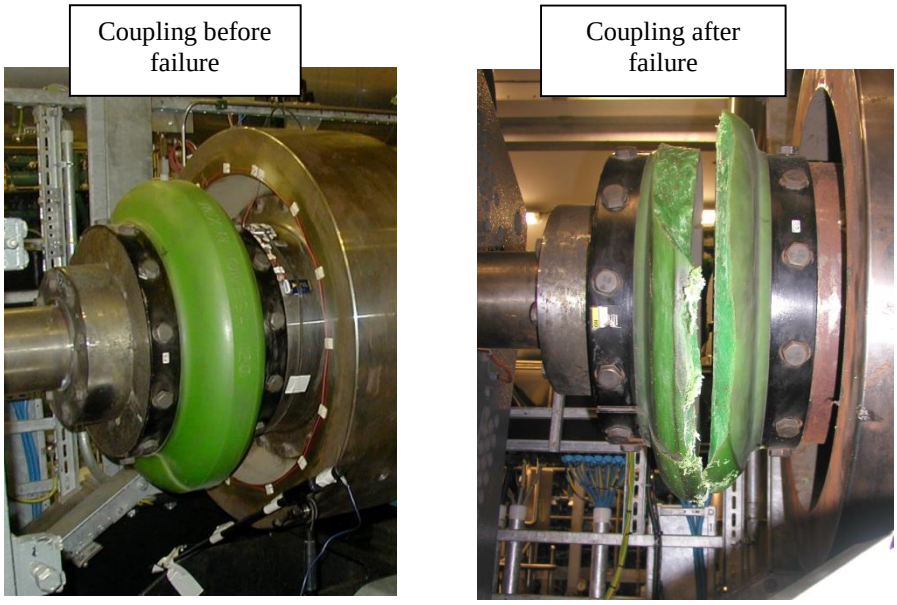

Figure 6: Picture of the elastic coupling before and after failure.

The plant operator replaced the coupling without any further modification and ran the drivetrain. The new coupling failed after three weeks of operation. Then, the controller of the active stepless suction valve unloader was modified and the coupling was replaced. The third coupling failed after a single day of operation.

The main task was to determine the particular cause of the drivetrain failure and to suggest an applicable solution. The drivetrain was investigated with main focus on the effect of the later installed active stepless suction valve unloading device. Part of the investigation was metrological and theoretical torsional vibration analysis of the drivetrain for different speeds and suction valve unloader positions.

5.2 Metrological analysis of the drivetrain

Strain gauges were applied on the motor stud to assess the operational torsional vibration of the drivetrain at the coupling. The measurement was carried out during unloaded compressor speed run-up from standstill to operating speed range as well as for different operation conditions.

The unloaded speed run-up showed the fundamental torsional natural frequency at 7.6 Hz. For loaded operation of the compressor, the effect of the active suction valve unloader showed an interesting character. Figure 7 illustrates the torque measured at the motor stud while increasing the position of the active stepless suction valve unloader from 15 % to 100 % at a constant motor speed of 600 rpm.

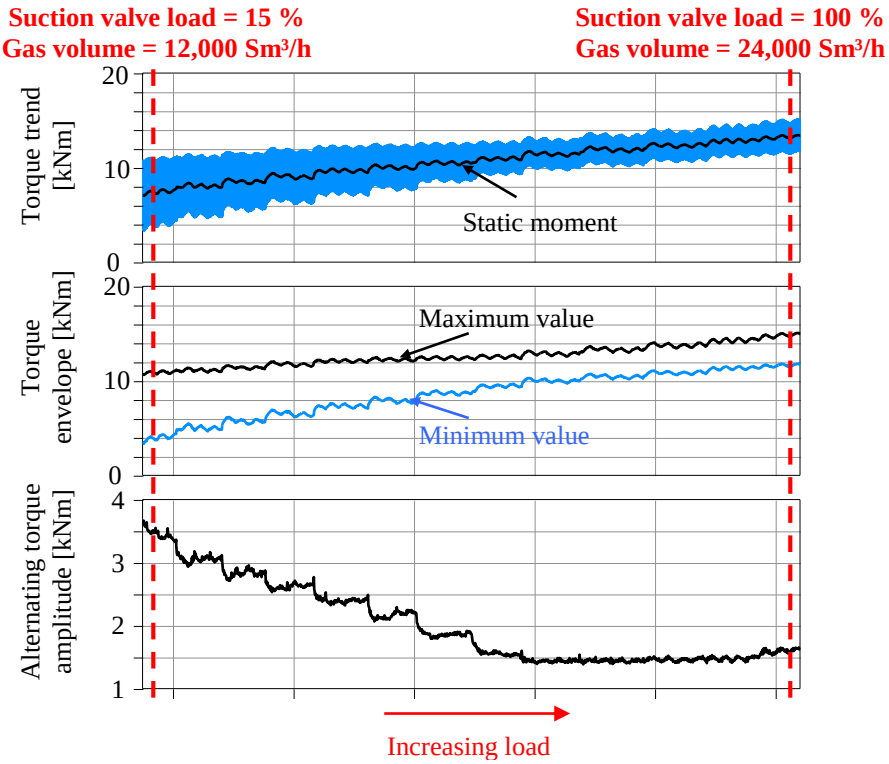

Figure 7: Measured torque for different discharge volumes controlled through the active stepless suction valve unloader at a motor speed of 600 rpm; top: measured torque trend (including the mean and alternating component), middle: maximum and minimum torque value, bottom: alternating torque amplitude.

As expected, the static torque increased with the discharge volume flow rate. As opposed to that, the alternating torque tended to decrease when the discharge volume increased. When the volume flow decreased by use of the active stepless suction valve unloader, the first order alternating stress component increased. This shows that the torsional loading of the drivetrain was indeed affected by the revamp.

The operational safety of the coupling can only be guaranteed when the measured/expected torsional loading is below the allowed loading recommended by the manufacturer. Unfortunately, the coupling manufacturer did not provide an explicit allowable value. Hence, the plant operator decided to use an alternative coupling that met the requirements of the extended operation condition.

5.3 Theoretical analysis of the drivetrain – Part 1

A finite-element-model of the drivetrain was developed as described in section 4. In order to validate the finite-element-model, the simulated results were compared with the measured results. Figure 8 shows the FE-model and the calculated natural frequencies with their corresponding mode shapes. The Campbell diagram (not displayed) of the drivetrain showed that the second torsional natural frequency interferes with the 9th to 15th harmonics.

In order to validate the FE-model, the fundamental torsional natural frequency and the forced response at the motor stud were compared with the measured results. The calculated torque on the motor stud while increasing the position of the active stepless suction valve unloader from 15 % to 100 % at a constant motor speed of 600 rpm is presented in figure 9. The comparison of the measured and the calculated fundamental torsional natural frequency and the torque levels and trends has shown the accuracy of the FE-model, the excitation torque and the assumed damping ratio of the system. But as stated in the previous section, it was not possible to suggest mitigation measures for the present drivetrain due to a lack of information on the allowable torque level from the coupling supplier.

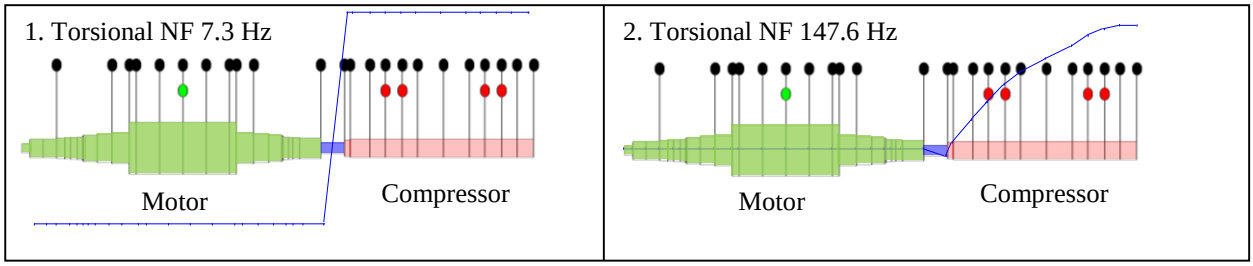

Figure 8: Calculated torsional natural frequency and corresponding mode shape for the drivetrain (motor: ▬ coupling: ▬ and crankshaft: ▬) – present.

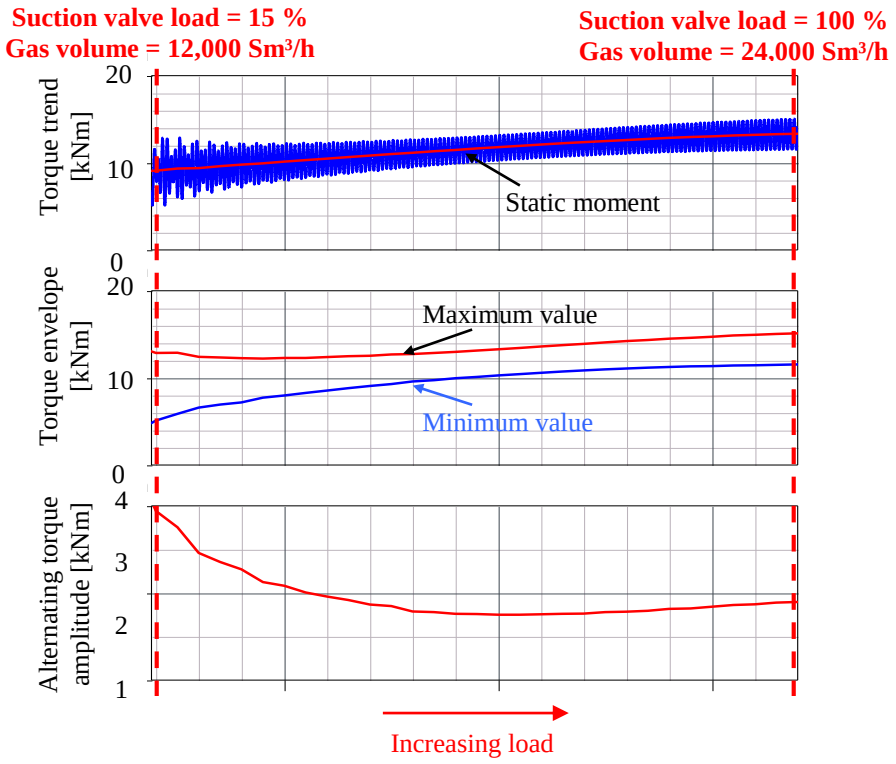

Figure 9: Calculated torque for different discharge volumes controlled through the active stepless suction valve unloader at a motor speed of 600 rpm, top: calculated torque trend (including the mean and alternating component), middle: maximum and minimum torque value, bottom: alternating torque amplitude.

5.4 Theoretical analysis of the drivetrain – Part 2

As stated in the previous section, the plant operator decided to replace the existing coupling with an alternative one that met the requirements of the extended operation condition from a list of available suppliers. Our initial analysis of the drivetrain with the selected coupling for the transmitted torque could not fulfill all the limits set by the supplier (for example the maximum torque level, heat dissipation etc.). Taking the practicability limitation set by the plant operator into account a new coupling along with a bigger flywheel was found to be applicable for the drivetrain with the planned extended discharge volume.

Figure 10 shows the calculated natural frequencies of the drivetrain with the new coupling. Here one can see that the first three natural frequencies of the drivetrain are torsional natural frequencies within the coupling in opposition to the original drivetrain where only one natural frequency was mainly in the coupling. This is due to the series arrangement of three rubber elements in the presently selected coupling whereas the original assembly had a single rubber element. The first torsional natural frequency moved from 7.6 Hz to 5.3 Hz and hence lay then significantly below the minimum operation speed of the new drivetrain. The fourth natural frequency, which was mainly torsional vibration of the crankshaft, remained at 147.6 Hz. Here again the Campbell diagram (not displayed) of the drivetrain showed that the fourth torsional natural frequency interfered with the 9^{th} to 15^{th} harmonics.

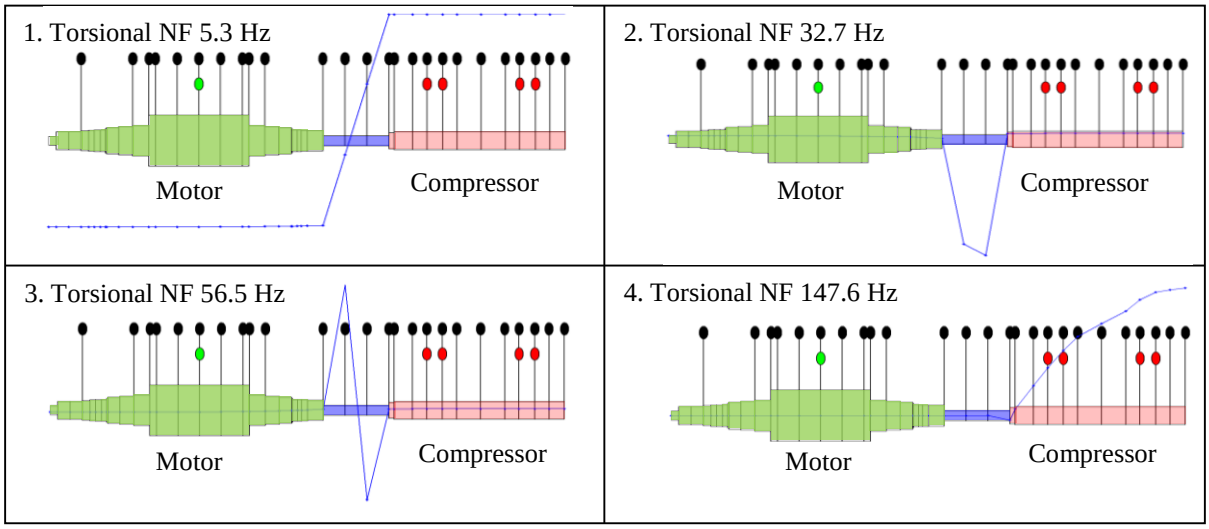

Figure 10: Calculated torsional natural frequency and corresponding mode shape for the drivetrain (motor: coupling: and crankshaft:) – recommended.

In order to determine the expected torsional vibration of the drivetrain through the compressor operation, an operational vibration analysis of the drivetrain in the time domain was conducted. Figure 11 shows the calculated torque of the coupling rubber elements for the actual and recommended coupling and flywheel. The calculation results show that the new coupling and flywheel reduces the load at the coupling. Hence, based on the simulation results a bigger flywheel and another rubber coupling were recommended. Until the coupling was modified as stated above, deactivating the active stepless suction valve unloader was recommended.

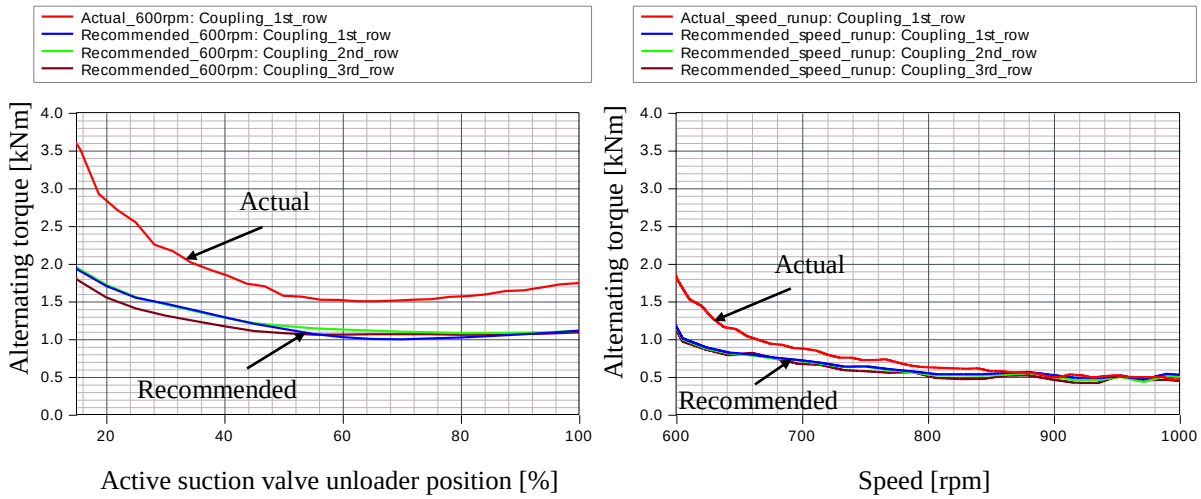

Figure 11: Comparison of the dynamic torque in the coupling for the drivetrain with the actual and the recommended coupling and flywheel, left: motor speed of 600 rpm for 15 % and 100 % volume flow, right: motor speed run-up from 600 rpm to 1,000 rpm with inactive suction valve unloader.

6 Possible mitigation methods for torsional vibration problem

In most cases the standards for reciprocating compressors demand to ensure a safety margin between natural frequencies and excitation frequencies. In the case of reciprocating compressors operating over a wide speed range, it is almost impossible to maintain the required safety margin to all excitation frequencies. At a minimum, the safety margin to the first order excitation with any of the natural frequencies in the operating speed range should then be maintained. Then a transient torsional analysis should be conducted to determine the transmitted dynamic torque and the resulting stress (static and fatigue) in all the elements considering the applicable stress concentration factor. In the case of rubber coupling and viscous torsional damper, the thermal power loss should also be calculated. The calculation results should be compared to material endurance limits, allowable coupling torque, allowable thermal load etc. If any of these values surpass the manufacturer limits, loaded operation of the compressor in the troublesome speed range (including a safety margin of 10 %) should be avoided.

In order to mitigate the torsional vibration problem during operation, continuous operation of the drivetrain at resonance should be avoided. A drivetrain can be revamped with a different coupling and flywheel to shift a torsional natural frequency to avoid operation at torsional resonance. It is advisable to undertake preventive maintenance of soft couplings and viscous damping to avoid drivetrain failure since they degrade with time. Full load run-up and shut-down of reciprocating compressor drivetrain leads to torsional overloading of sensitive parts and should be avoided.

7 Conclusion

Torsional vibration at reciprocating compressors cannot be identified on site with simple measuring methods like e. g. measurement of the casing vibration. Often high torsional dynamic stress is not recognised until damages appear. Hence, it is advisable to conduct a detailed torsional vibration analysis when planning a new drivetrain or modifying an existing one. There are different methods to influence the torsional vibration behaviour of a reciprocating compressor. We recommend to check the results of the analysis by measurement to ensure the safety of the plant. From the torsional loading point of view, a trouble-free operation of the compressor system can be ensured by a combination of calculation and measurement.

References

[1] API Publication 684 (2005): *Tutorial on the API Standard paragraphs covering rotor dynamics and balancing: An introduction to lateral critical and train torsional analysis and rotor balancing.* American Petroleum Institute, Washington, D.C.

[2] Argyris, J., Mlejnek, H.P. (1986): *Die Methode der Finiten Elemente*. Band I-III, Friedr. Vieweg & Sohn, Braunschweig.

[3] Childs, D. (1993): *Turbomachinery Rotordynamics.* Wiley-Intersciences, New York.

[4] Corbo, M.A. and Malanoski, S.B. (1996): Practical design against torsional vibration. *Proceedings of the twenty-fifth turbomachinery symposium*, College Station, Texas, Sept., pp. 189–222.

[5] Dukkipati, R.V. (2009): *MATLAB for Mechanical Engineers*. New Age Science Limited, UK.

[6] Feese, T. and Hill, C. (2009): Prevention of torsional vibration problems in reciprocating machinery. *Proceedings of the thirty-eighth turbomachinery symposium*, Houston, Texas, Sept. 14-17, pp. 213–238.

[7] Frenkel, M. I. (1969): *Kolbenverdichter.* VEB Verlag Technik, Berlin.

[8] Irretier, H. (2007): *Maschinen- und Rotordynamik: Lecture Manuscript*. 5th edition. Institute of Mechanics, University of Kassel, Kassel.

[9] Isakower, R.I. (1979): *Design charts for torsional properties of non-circular shafts.* Final technical report ARMID-TR-78001, US Army Armament research and development command, NJ.

[10] Nestorides, E.J.(1958): *Handbook of Torsional Vibration*. B.I.C.E.R.A. Cambridge University Press, New York.

[11] Tondl, A. (1965): *Some Problems of Rotordynamics*. Chapman and Hall, London.

[12] Wachel,J. C. and Szenasi, F. R. (1993): Analysis of torsional vibration in rotating machinery. *Proceedings of the twenty-second turbomachinery symposium*, College Station, Texas, Sept. 14-16, pp. 127–152.